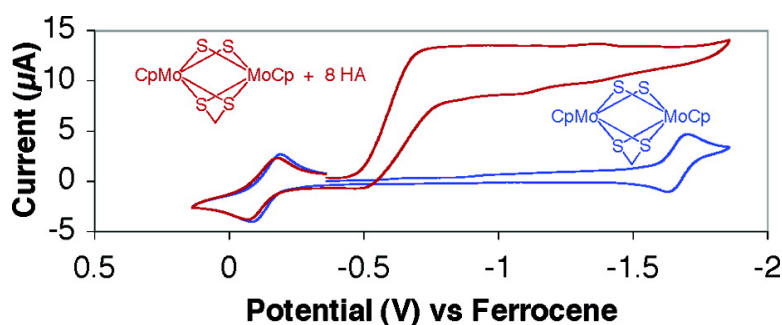


## Molybdenum–Sulfur Dimers as Electrocatalysts for the Production of Hydrogen at Low Overpotentials

Aaron M. Appel, Daniel L. DuBois, and M. Rakowski DuBois

*J. Am. Chem. Soc.*, **2005**, 127 (36), 12717-12726 • DOI: 10.1021/ja054034o • Publication Date (Web): 19 August 2005

Downloaded from <http://pubs.acs.org> on March 25, 2009



### More About This Article

Additional resources and features associated with this article are available within the HTML version:

- Supporting Information
- Links to the 10 articles that cite this article, as of the time of this article download
- Access to high resolution figures
- Links to articles and content related to this article
- Copyright permission to reproduce figures and/or text from this article

[View the Full Text HTML](#)

## Molybdenum–Sulfur Dimers as Electrocatalysts for the Production of Hydrogen at Low Overpotentials

Aaron M. Appel,<sup>†</sup> Daniel L. DuBois,<sup>\*,†,‡</sup> and M. Rakowski DuBois<sup>\*,†</sup>

Contribution from the Department of Chemistry and Biochemistry, University of Colorado, Boulder, Colorado 80309, and National Renewable Energy Laboratory, 1617 Cole Boulevard, Golden, Colorado 80401

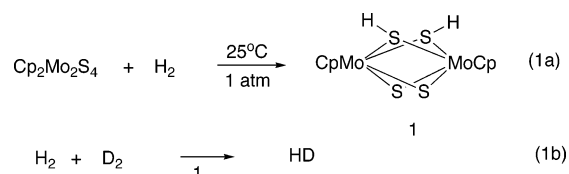
Received June 17, 2005; E-mail: Mary.Rakowski-DuBois@colorado.edu; Dan\_DuBois@nrel.gov

**Abstract:** (CpMo $\mu$ -S)<sub>2</sub>S<sub>2</sub>CH<sub>2</sub>, **2**, and related derivatives serve as electrocatalysts for the reduction of protons with current efficiencies near 100%. The kinetics of the electrochemical reduction process has been studied, and the effects of varying the proton source, the solvent, the cyclopentadienyl substituents, and the sulfur substituents on the catalyst have been examined. The reduction of excess *p*-cyanoanilinium tetrafluoroborate under a hydrogen atmosphere in 0.3 M Et<sub>4</sub>NBF<sub>4</sub>/acetonitrile buffered at pH 7.6 is catalyzed by **2** at –0.64 V versus ferrocene, with an overpotential of 120 mV. Protonation of the sulfido ligand in **2** is an initial step in the catalytic process, and the rate-determining step at high acid concentrations appears to be the elimination of dihydrogen. The elimination may occur either from adjacent hydrosulfido sites or from a hydrosulfido–molybdenum hydride intermediate.

### Introduction

The production of hydrogen from electricity and its reverse reaction, the oxidation of hydrogen, are important components in developing a hydrogen-based energy delivery system. Catalytic reactions involving the formation or consumption of hydrogen are frequently associated with transition metal centers in which d-orbitals play a key role in H–H bond formation or cleavage via oxidative addition/reductive elimination mechanisms. However, there is a large body of evidence that for certain classes of compounds, the ligands play an important role in hydrogen activation. Many examples of metal complexes with nitrogen, sulfur and, less frequently, oxygen donor ligands that function as a proton acceptor in the heterolytic activation of hydrogen have been reported.<sup>1–9</sup> In many cases, these reactions are proposed to involve a [2 + 2] addition of hydrogen across

the metal–ligand bond. Recently, examples of [3 + 2] hydrogen addition to cis-oxo ligands in high valent metal complexes have been reported to occur without direct participation of the metal ion.<sup>10</sup>



In earlier work, we reported the addition of hydrogen to bridging sulfido ligands in a molybdenum dimer to give a bis(hydrosulfido) complex, **1**.<sup>11</sup> Although further hydrogen addition to the sulfido ligands in **1** does not produce a stable or detectable tetrakis(hydrosulfido) product, **1** was found to catalyze HD formation from a H<sub>2</sub>/D<sub>2</sub> mixture.<sup>12</sup> A pathway was proposed that involved direct hydrogen addition to the lowest unoccupied molecular orbital or LUMO of **1**. The LUMOs of **1** as well as that of the related complex (CpMo  $\mu$ -S)<sub>2</sub>(S<sub>2</sub>CH<sub>2</sub>), **2**, contain significant sulfur character and are of proper symmetry to act as acceptor orbitals for  $\pi$  bonds of olefins or  $\sigma$  bonds of hydrogen.<sup>13</sup> The reaction of **1** with olefins resulted in the formation of a bis(dithiolate) complex with the elimination of

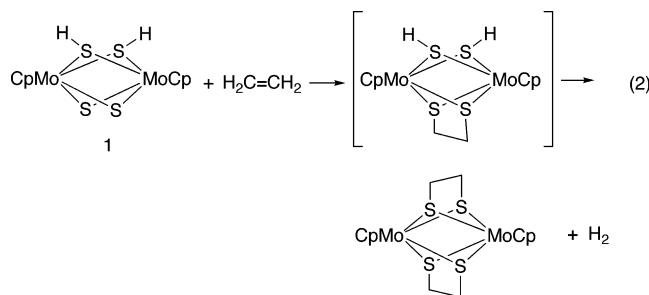
<sup>†</sup> University of Colorado.

<sup>‡</sup> National Renewable Energy Laboratory.

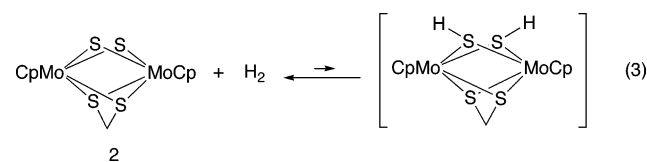
- (1) Howard, W. A.; Waters, M.; Parkin G. *J. Am. Chem. Soc.* **1993**, *115*, 4917. (b) Howard, W. A.; Trnka, T. M.; Waters, M.; Parkin, G. *J. Organomet. Chem.* **1997**, *528*, 95.
- (2) Sweeney, Z. K.; Polse, J. L.; Andersen, R. A. Bergman, R. G.; Kubinec, M. G. *Organometallics* **1999**, *18*, 5502.
- (3) Linck, R. C.; Pafford, R. J.; Rauchfuss, T. B. *J. Am. Chem. Soc.* **2001**, *123*, 8856.
- (4) Ohki, Y.; Matsuura, N.; Marumoto, T.; Kawaguchi, H.; Tatsumi, K. *J. Am. Chem. Soc.* **2003**, *125*, 7978.
- (5) Hanna, T. E.; Keresztes, I.; Lobkovsky, E.; Bernskoetter, W. H.; Chirik, P. *J. Organometallics* **2004**, *23*, 3448.
- (6) Sandoval, C. A.; Ohkuma, T.; Muniz, K.; Noyori, R. *J. Am. Chem. Soc.* **2003**, *125*, 13490.
- (7) (a) Abdur-Rashid, K.; Clapham, S. E.; Hadzovic, A.; Harvey, J. N.; Lough, A. J.; Morris, R. H. *J. Am. Chem. Soc.* **2002**, *124*, 15104. (b) Li, T.; Churlaud, R.; Lough, A. J.; Abdur-Rashid, K.; Morris, R. H. *Organometallics* **2004**, *23*, 6239. (c) Morris, R. H. *Organometallics* **2005**, *24*, 479. (d) Morris, R. H. *J. Am. Chem. Soc.* **2005**, *127*, 1870.
- (8) (a) Casey, C. P.; Johnson, J. B.; Singer, S. W.; Cui, Q. *J. Am. Chem. Soc.* **2005**, *127*, 3100. (b) Casey, C. P.; Singer, S. W.; Powell, D. R.; Hayashi, R. K.; Kavana, M. *J. Am. Chem. Soc.* **2001**, *123*, 1090.
- (9) Ito, M.; Hirakawa, M.; Murata, K.; Ikariya, T. *Organometallics* **2001**, *20*, 379. (b) Ito, M.; Hirakawa, M.; Osaku, A.; Ikariya, T. *Organometallics* **2003**, *22*, 4190.

- (10) (a) Collman, J. P.; Slaughter, L. M.; Eberspacher, T. S.; Strassner, T.; Brauman, J. I. *Inorg. Chem.* **2001**, *40*, 6272. (b) Dehestani, A.; Lam, W. H.; Hrovat, D. A.; Davidson, E. T.; Borden, W. T.; Mayer, J. M. *J. Am. Chem. Soc.* **2005**, *127*, 3423.
- (11) Casewit, C. J.; Coons, D. E.; Wright, L. L.; Miller, W. K.; Rakowski DuBois, M. *Organometallics* **1986**, *5*, 91.
- (12) Rakowski DuBois, M.; VanDerveer, M. C.; DuBois, D. L.; Haltiwanger, R. C.; Miller, W. K. *J. Am. Chem. Soc.* **1980**, *102*, 7456.
- (13) DuBois, D. L.; Miller, W. K.; Rakowski DuBois, M. *J. Am. Chem. Soc.* **1981**, *103*, 3429. (b) Bursten, B. E.; Cayton, R. H. *Inorg. Chem.* **1989**, *28*, 2846. (c) Tremel, W.; Hoffman, R.; Jemmes, E. D. *Inorg. Chem.* **1989**, *28*, 1213.

hydrogen (eq 2).<sup>12</sup> The observation that hydrogen is formed in this reaction is interesting, because it implies a facile elimination of hydrogen from adjacent hydrosulfido ligands in an undetected intermediate Mo(III)/(III) complex containing one dithiolate bridge. Complex **2** also reacts reversibly with olefins to form the corresponding dithiolate complex.<sup>14</sup> However, consistent with the previous proposal, the addition of hydrogen (1–2 atm) to the sulfido ligands in **2** is not detected by NMR spectroscopy (eq 3), although **2** does function as a hydrogenation catalyst for certain substrates.<sup>11</sup>

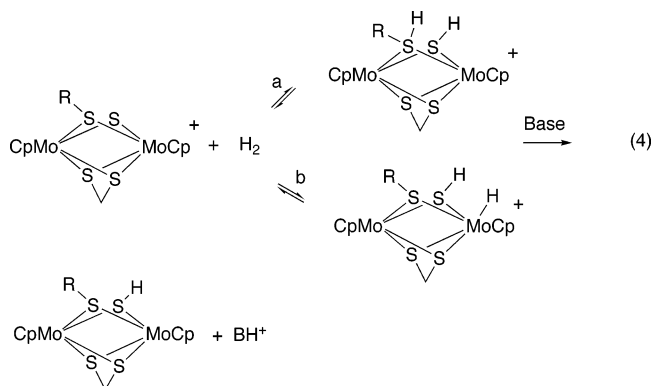


Cationic derivatives of the molybdenum sulfide dimers have also been found to react with hydrogen<sup>15,16</sup> (e.g., reaction 4). The reaction may involve homolytic cleavage through the addition of hydrogen to the LUMO of the molybdenum cation, which has significant sulfur character, pathway a. Alternatively, the reaction could involve the heterolytic cleavage of hydrogen, with the LUMO serving as a hydride acceptor site, and the HOMO, which is an antibonding metal-based  $\delta^*$  orbital with almost no sulfur character, acting as a base, pathway b. In the latter case, the roles normally assigned to transition metals and their associated ligands in hydrogen activation would be reversed. The sulfur atom acts as the hydride acceptor, and the metal site serves as a proton acceptor. We note that analogous homolytic and heterolytic hydrogen activation pathways have also been considered for unpromoted and Co- or Ni-promoted molybdenum sulfide surfaces.<sup>17</sup>



Indirect support for pathway b in eq 4 was obtained from studies of nucleophilic and electrophilic addition to related dimers. For example, in studies of the cationic derivatives, the sulfido ligand has been observed to add other nucleophiles (e.g.,

alkylation with alkyl-lithium reagents).<sup>18</sup> In protonation studies of certain neutral molybdenum complexes,  $(\text{CpMo})_2(\text{S}_2\text{CH}_2)(\text{SR})_2$ , carried out at low temperatures, NMR evidence was observed for the formation of unstable molybdenum hydride products.<sup>19</sup>



In addition to their ability to undergo facile reactions with hydrogen, both neutral and cationic derivatives exhibit well-behaved electrochemical properties, undergoing reversible electrochemical reductions without significant structural changes.<sup>18</sup> The extensive chemistry suggesting facile addition and elimination of hydrogen from these molybdenum sulfur dimers and their electrochemical properties has led us to investigate more fully the potential of this class of complexes as electrocatalysts for hydrogen production/oxidation reactions. Many metallocosulfur complexes are known to serve as catalysts for proton reduction. In particular, the binuclear active sites in the hydrogenase enzymes<sup>20</sup> and synthetic models that involve binuclear iron complexes bridged by dithiolate ligands<sup>21–25</sup> have been the focus of intense study. We report here that complex **2** and related derivatives function as electrocatalysts for hydrogen production. These dinuclear molybdenum systems are distinguished by high current efficiencies and exceptionally low overpotentials, and they involve protonation of sulfido ligands as a critical part of the catalytic cycle. Aspects of the sulfur-based mechanism are discussed.

## Results

**Electrochemical Studies.** A cyclic voltammogram of **2** in acetonitrile is shown in the red (bottom) trace in Figure 1. A reversible one-electron reduction is observed at  $-1.66$  V versus

- (14) McKenna, M.; Wright, L. L.; Miller, D. J.; Tanner, L.; Haltiwanger, R. C.; Rakowski DuBois, M. *J. Am. Chem. Soc.* **1983**, *105*, 5329.  
 (15) (a) Laurie, J. C. V.; Duncan, L.; Haltiwanger, R. C.; Weberg, R. T.; Rakowski DuBois, M. *J. Am. Chem. Soc.* **1986**, *108*, 6234. (b) Weberg, R. T.; Haltiwanger, R. C.; Laurie, J. C. V.; Rakowski DuBois, M. *J. Am. Chem. Soc.* **1986**, *108*, 6242.  
 (16) (a) Lopez, L. L.; Bernatis, P.; Birnbaum, J.; Haltiwanger, R. C.; Rakowski DuBois, M. *Organometallics* **1992**, *11*, 2424. (b) Lopez, L. L.; Godziela, G.; Rakowski DuBois, M. *Organometallics* **1991**, *10*, 2660.  
 (17) (a) Travert, A.; Nakamura, H.; van Santen, R. A.; Cristol, S.; Paul, J. F.; Payen, E. *J. Am. Chem. Soc.* **2002**, *124*, 7084. (b) Byskov, L. S.; Bollinger, M.; Norskov, J. K.; Clausen, B. S.; Topsoe, H. *J. Mol. Catal.* **2000**, *163*, 117. (c) Thomas, C.; Vivier, L.; Lemberton, J. L.; Kasztelan, S.; Perot, G. *J. Catal.* **1997**, *167*, 1. (d) Thomas, C.; Viveier, L.; Travert, A.; Mauge, F.; Kasztelan, S.; Perot, G. *J. Catal.* **1998**, *179*, 495. (e) Anderson, A. B.; Al-Saigh, Z. Y.; Hall, W. K. *J. Phys. Chem.* **1988**, *92*, 803. (f) Hinnemann, B.; Moses, P. G.; Bonde, J.; Jorgensen, K. P.; Nielsen, J. H.; Horch, S.; Chorkendorff, I.; Norskov, J. K. *J. Am. Chem. Soc.* **2005**, *127*, 5308.

- (18) Casewit, C. J.; Haltiwanger, R. C.; Noordik, J.; Rakowski DuBois, M. *Organometallics* **1985**, *4*, 119.  
 (19) Bernatis, P.; Haltiwanger, R. C.; Rakowski DuBois, M. *Organometallics* **1992**, *11*, 2435.  
 (20) Leger, C.; Jones, A. K.; Roseboom, W.; Albracht, S. P. J.; Armstrong, F. A. *Biochem.* **2002**, *41*, 15736. (b) Darensbourg, M. Y.; Lyon, E. J.; Smees, J. J. *Coord. Chem. Rev.* **2000**, *206–207*, 533. (c) Nicolet, Y.; Cavazza, C.; Fontecilla-Camps, J. C. *J. Inorg. Biochem.* **2002**, *91*, 1. (d) Bruschi, M.; Fantucci, P.; De Gioia, L. *Inorg. Chem.* **2002**, *41*, 1421.  
 (21) (a) Gloaguen, F.; Lawrence, J. D.; Rauchfuss, T. B. *J. Am. Chem. Soc.* **2001**, *123*, 9476. (b) Gloaguen, F.; Lawrence, J. D.; Rauchfuss, T. B.; Benard, M.; Rohmer, M. M. *Inorg. Chem.* **2002**, *41*, 6573.  
 (22) Ott, S.; Kritikos, M.; Akermark, B.; Su, L.; Lomoth, R. *Angew. Chem., Int. Ed.* **2004**, *43*, 1006.  
 (23) (a) Capon, J. F.; Gloaguen, F.; Schollhammer, P.; Talarmin, J. J. *Electroanal. Chem.* **2004**, *566*, 241. (b) Capon, J. F.; Hassnaoui, S. E.; Gloaguen, F.; Schollhammer, P.; Talarmin, J. *Organometallics* **2005**, *24*, 2020.  
 (24) Mejia-Rodriguez, R.; Chong, D.; Reibenspies, J. H.; Soriaga, M. P.; Darensbourg, M. Y. *J. Am. Chem. Soc.* **2004**, *126*, 12004.  
 (25) (a) Tard, C.; Liu, X.; Ibrahim, S. K.; Bruschi, M.; DeGiola, L.; Davies, S. C.; Yang, X.; Wang, L. S.; Sawers, G.; Pickett, C. J. *Nature* **2005**, *433*, 610. (b) Tard, C.; Liu, X.; Hughes, K. L.; Pickett, C. J. *J. Chem. Soc., Chem. Commun.* **2005**, 133.

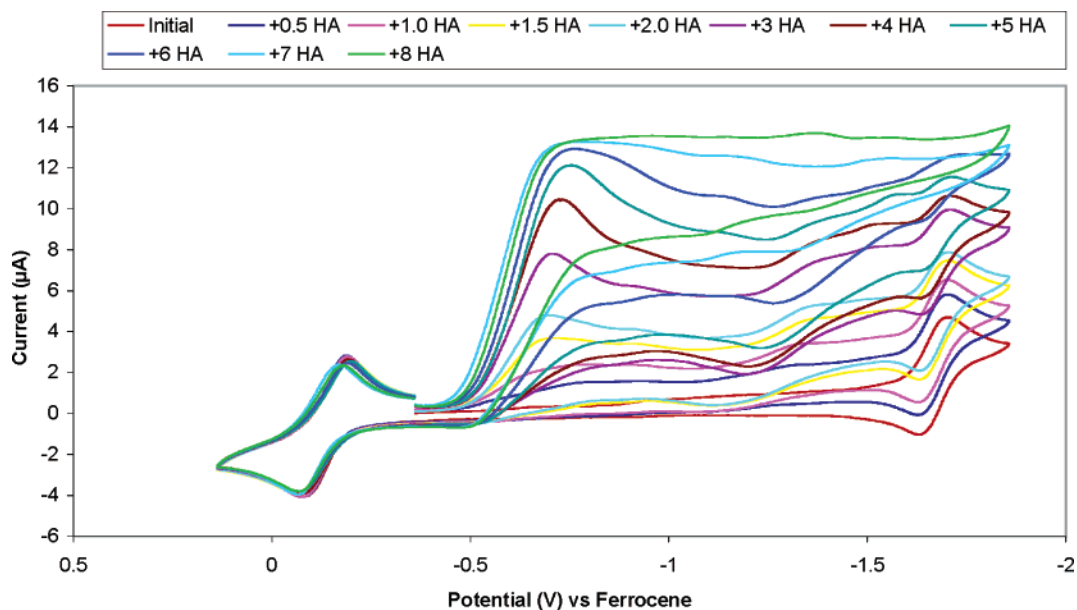


**Figure 1.** Cyclic voltammograms of  $(\text{CpMoS})_2\text{S}_2\text{CH}_2$ , **2** (0.95 mM), as a function of *p*-cyanoanilinium tetrafluoroborate concentration (expressed as equiv) recorded in 0.3 M  $\text{Et}_4\text{NBF}_4$ /acetonitrile solution at a glassy carbon electrode at 50 mV/s.

ferrocene, and the quasi-reversible one electron oxidation occurs at  $-0.08$  V. Upon addition of 1 equiv of *p*-cyanoanilinium tetrafluoroborate as the acid, a new irreversible reduction wave is observed near  $-0.7$  V versus the ferrocene/ferrocenium couple. Further addition of acid results in an additional positive shift in potential, an increase in the peak current, and a flattening of the wave, consistent with a catalytic process.<sup>26</sup> However, increasing the acid concentration above ca. 8 equiv resulted in no further current enhancement. With 8 equiv of acid, the plateau current is nearly independent of the scan rate (20–200 mV/s), another feature expected for a catalytic process<sup>26</sup> (see Figure S1 of Supporting Information). To confirm that the product of this reaction was  $\text{H}_2$  gas, a controlled-potential electrolysis of a solution of **2** containing 29 equiv of *p*-cyanoanilinium tetrafluoroborate was performed in a closed cell. After passing 52.8 C of charge at  $-0.96$  V versus Fc, a sample of the gas was withdrawn and analyzed and quantified by gas chromatography. The amount of hydrogen (0.27 mmol, 10.6 mol of  $\text{H}_2$  per mol of catalyst) was determined by integration, and a current efficiency of  $98 \pm 5\%$  for hydrogen production was calculated assuming that two electrons are required for each  $\text{H}_2$  molecule produced.

**Kinetic Studies of the Catalytic Reaction.** For a reversible electron-transfer reaction followed by a fast catalytic reaction (i.e., an  $\text{E}_\text{R}\text{C}_\text{cat}$  scheme), the catalytic current is given by eq 5.<sup>26</sup> In eq 5,  $n$  is the number of electrons involved in the catalytic process (2 for  $\text{H}_2$  production);  $F$  is the Faraday constant;  $A$  is the area of the electrode;  $D$  is the diffusion coefficient of the catalyst;  $k$  is the rate constant for the catalytic reaction;  $[Q]$  is the concentration of the substrate (acid in this case); and  $y$  is the order of the catalytic reaction in substrate. The derivation of eq 5 assumes that the reaction is first order in catalyst and that the concentration of the substrate is large as compared to the concentration of the catalyst so that its concentration is nearly

unchanged during the scan.<sup>26</sup> Under these conditions, pseudo-first-order kinetics apply.

$$i_c = nFA[\text{cat}](Dk[Q]^y)^{1/2} \quad (5)$$

As shown in Figure 2, the catalytic current initially increases in a linear fashion with acid concentration and then levels off or decreases slightly after ca. 8 equiv have been added. The linear dependence of the catalytic current on acid concentration at low acid concentrations is consistent with either a rate-determining step that is second order in acid (see eq 5) or with a preequilibrium involving proton addition to **2** followed by electron transfer and a catalytic reaction. At higher acid concentrations, the catalytic current is independent of acid concentration. This observation is consistent with hydrogen elimination as the rate-determining step at high acid concentrations. From eq 5, it can also be seen that the catalytic current does not exhibit the square root dependence on catalyst concentration that is observed for substrate concentrations but rather is directly proportional to this concentration. A plot of the catalytic current versus catalyst concentration is shown in Figure 3, and it is best fit by a straight line, indicating a first-order dependence on catalyst.

A value for the product  $AD^{1/2}$  of eq 5 can be easily obtained from the peak current observed by cyclic voltammetry for the catalyst in the absence of acid using the same electrode. Using this value, eq 5 can be used to calculate a third-order rate constant from the currents observed at low acid concentrations ( $y = 2$ ) and a first-order rate constant from the currents observed at high acid concentrations ( $y = 0$ ). The best fit line at low acid concentrations (see first six data points of Figure 2) gives a third-order rate constant of  $3.7 \times 10^4 \text{ M}^{-2} \text{ s}^{-1}$ , and the average value of the current at high concentrations gives a first-order rate constant for  $\text{H}_2$  elimination of  $1.5 \pm 0.3 \text{ s}^{-1}$ . The third-order rate constant is undoubtedly a composite of equilibrium constants and rate constants and as such does not reflect the kinetics of a fundamental step. However, the first-order rate constant should reflect the true rate of  $\text{H}_2$  loss from the catalytic intermediate.

(26) (a) Bard, A. J.; Faulkner, L. R. *Electrochemical Methods*; Wiley: New York, 1980; pp 555–559. (b) Delahay, P.; Stiehl, G. L. *J. Am. Chem. Soc.* **1952**, *74*, 3500–3505. (c) Nicholson, R. S.; Shain, I. *Anal. Chem.* **1964**, *36*, 706. (d) Saveant, J. M.; Vianello, E. *Electrochim. Acta* **1965**, *10*, 905–920. (e) *Ibid* **1967**, *12*, 629–646.

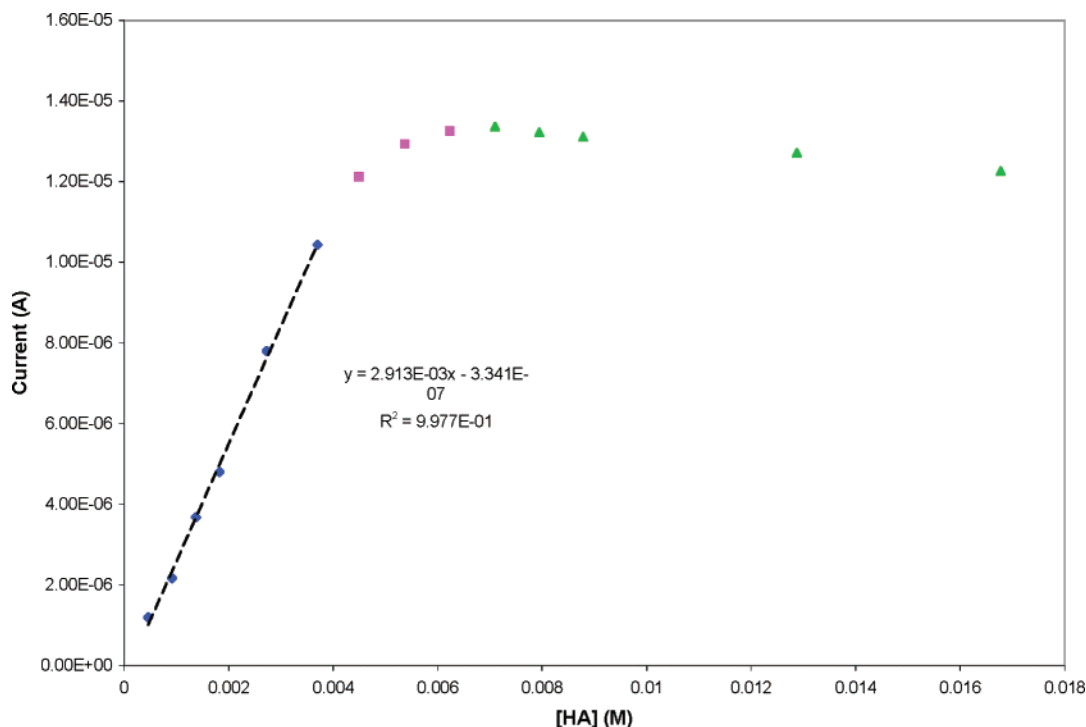


**Figure 2.** Dependence of the catalytic current of  $(\text{CpMoS})_2\text{S}_2\text{CH}_2$ , **2** (0.95 mM), on *p*-cyanoanilinium concentration recorded in 0.3 M  $\text{Et}_4\text{NBF}_4$ /acetonitrile solution at a glassy carbon electrode at 50 mV/s. The average value of the current at high acid concentrations gives a first-order rate constant of  $1.5 \pm 0.3 \text{ s}^{-1}$ .

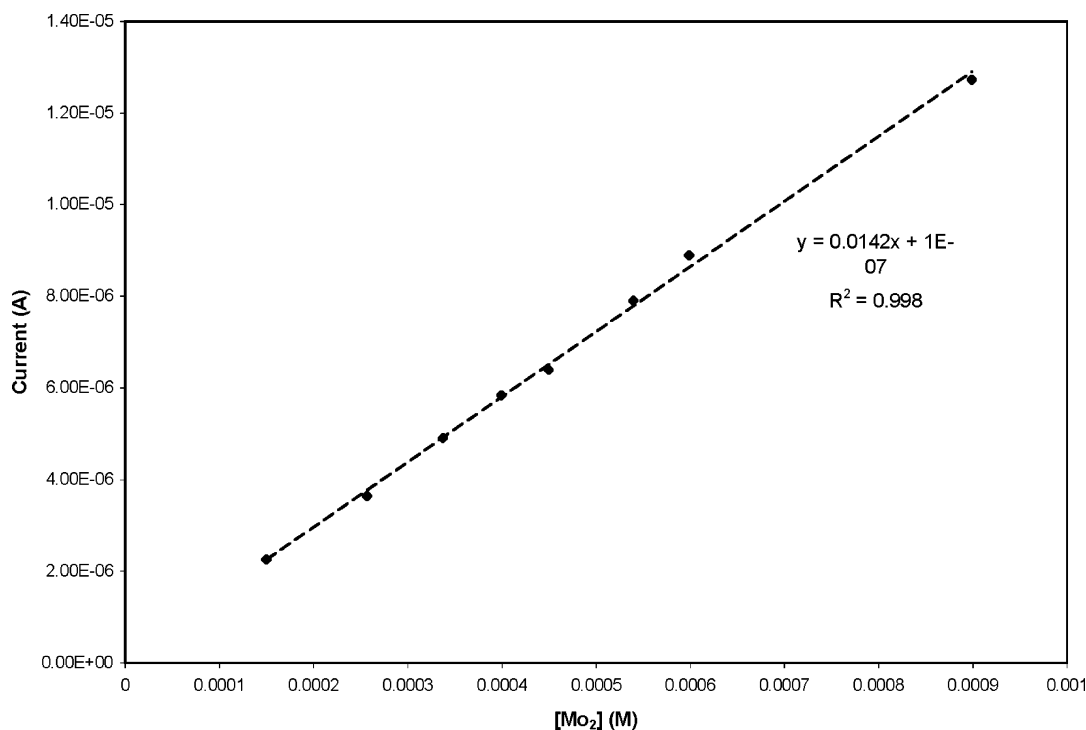


**Figure 3.** Dependence of catalytic current on concentration of catalyst,  $(\text{CpMoS})_2\text{S}_2\text{CH}_2$ , **2**, as catalyst is added to 9.5 mM *p*-cyanoanilinium tetrafluoroborate recorded in 0.3 M  $\text{Et}_4\text{NBF}_4$ /acetonitrile solution at a glassy carbon electrode at 50 mV/s.

**Catalyst Sensitivity to Carbon Monoxide.** To probe the influence that CO would have on the catalytic rate, cyclic voltammograms were recorded on acidic solutions of **2** that had been purged with pure carbon monoxide, Figure 4. At relatively low concentrations of acid (2 and 5 equiv of *p*-cyanonilinium ion) the catalytic current is about 50% of that observed in the absence of CO. The mechanism by which CO inhibits the proton reduction is not known. Measurable binding of CO by **2** does

not occur, but spectroscopic evidence for a slow reaction of **2** with CO in the presence of acid in acetonitrile has been observed. Further work will be necessary to identify the product (but it does not appear to be the formylthiolate derivative resulting from CO insertion into the S–H bond of protonated **2**). At 20 equiv of the acid, the ratio of catalytic current,  $i_{\text{cat}}$ , to the cathodic peak current in the absence of acid,  $i_p$  (a measure of the catalytic efficiency), is 2.1 under CO or approximately

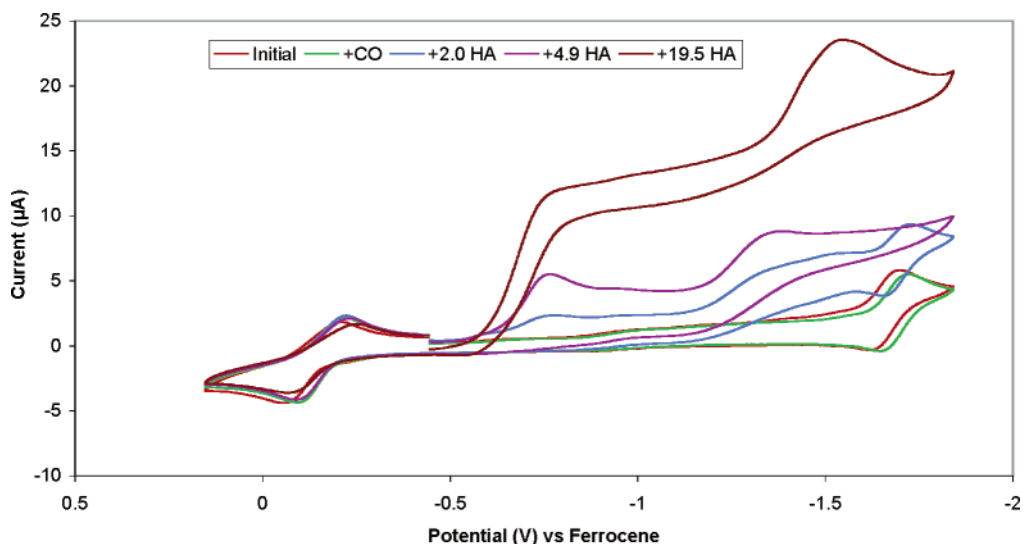
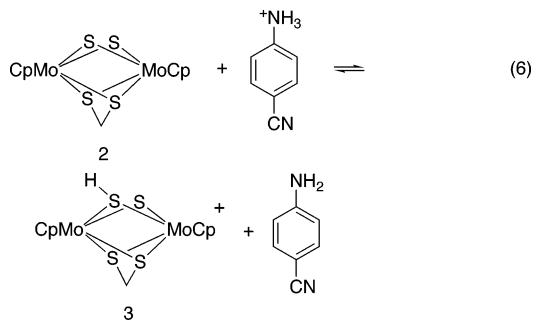


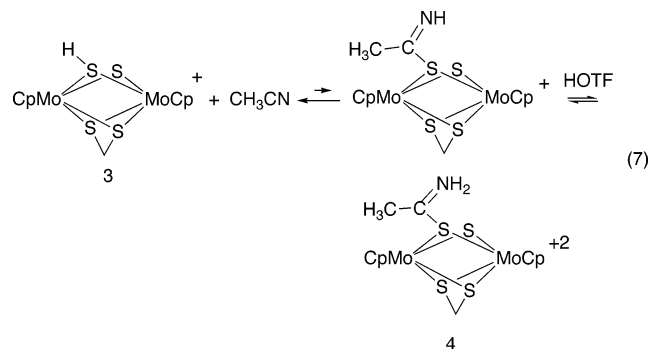
**Figure 4.** Cyclic voltammograms of  $(\text{CpMoS})_2\text{S}_2\text{CH}_2$  (0.95 mM) as a function of *p*-cyanoanilinium tetrafluoroborate concentration under a CO atmosphere recorded in 0.3 M  $\text{Et}_4\text{NBF}_4$ /acetonitrile solution at a glassy carbon electrode at 50 mV/s. The large irreversible wave with  $E_p = -1.6$  V is assigned, on the basis of control experiments, to the direct reduction of *p*-cyanoanilinium at the glassy carbon electrode.

80% of that observed under nitrogen. It is apparent that  $\text{H}_2$  production continues at a significant rate even in the presence of a very large amount of CO, and the potential at which hydrogen production occurs is not significantly affected. As the acid concentration is increased, two additional irreversible reduction waves are observed in Figure 4 at  $E_p = -1.35$  V and  $E_p = -1.6$  V. The latter wave is assigned on the basis of control experiments to the direct reduction of *p*-cyanoanilinium at the glassy carbon electrode. The reduction wave with  $E_p$  at  $-1.35$  V (5 equiv of acid) has not been assigned.



**Stoichiometric Reactions of 2 with Acid.** Previous studies have shown that the protonation of **2** with 1 equiv of triflic acid in acetonitrile produces the red hydrosulfido complex  $[(\text{CpMo})_2(\mu\text{-SH})(\mu\text{-S})(\text{S}_2\text{CH}_2)]\text{OTf}$ , **3**, which has been isolated and characterized.<sup>27</sup> At scan rates of 3.2 V/s, two quasi-reversible reduction waves are observed for **3** at  $-0.56$  ( $\Delta E_p = 197$  mV) and  $-1.22$  V versus Fc ( $\Delta E_p = 180$  mV) (Figure S2). The proton addition is a reversible reaction, and deprotonation of **3** results in a rapid color change from red to blue and the regeneration of **2**. With a 10-fold excess of a 2:1 mixture of *p*-cyanoanilinium tetrafluoroborate and *p*-cyanoaniline, equilibrium is observed by NMR spectroscopy. Rapid proton exchange between **2** and **3** is observed, and determination of the average chemical shifts led to a  $K_{\text{eq}}$  value of 0.3 for reaction 6. The addition of  $\log K_{\text{eq}}$  (6) to the  $\text{p}K_{\text{a}}$  of *p*-cyanoanilinium in

acetonitrile (7.6)<sup>28</sup> gives a  $\text{p}K_{\text{a}}$  of  $7.1 \pm 0.3$  for **3** in acetonitrile at 20 °C. This value is similar to our previously reported  $\text{p}K_{\text{a}}$  for **3** determined by visible spectroscopy of a 1:1 ratio of **2** and 2,4-dichloroanilinium ion.<sup>27</sup> In acetonitrile, **3** reacts with one additional equiv of triflic acid to give a near quantitative yield of **4**, in which acetonitrile has inserted into the SH bond to form an iminothiolate ligand. Protonation of the iminothiolate ligand is necessary to shift this equilibrium to the right (eq 7). Complex **4** has been isolated and characterized previously.<sup>29</sup> This reaction is also reversible, and treatment of **4** with base regenerates first **3** then **2**. We have repeated these studies using an excess ( $>4$  equiv) of *p*-cyanoanilinium as the acid. In this case, reversible formation of **3** is observed by <sup>1</sup>H NMR spectroscopy, but formation of **4** is not detected. The formation of **4** apparently requires a stronger acid than *p*-cyanoanilinium tetrafluoroborate.



**Acid Dependence of the Catalytic Reaction.** The electrocatalytic activity of the protonated dimer **3** for proton reduction in acetonitrile has been studied with three different acids. As discussed in the previous paragraph, the  $\text{p}K_{\text{a}}$  of **3** is  $7.1 \pm 0.3$  in acetonitrile. In comparison, triflic acid, *p*-cyanoanilinium tetrafluoroborate, and bromoanilinium tetrafluoroborate have  $\text{p}K_{\text{a}}$

(27) Birnbaum, J.; Godziela, G.; Maciejewski, M.; Tonker, T. L.; Haltiwanger, R. C.; Rakowski DuBois, M. *Organometallics* **1990**, *9*, 394.

(28) Edidin, R. T.; Sullivan, J. M.; Norton, J. R. *J. Am. Chem. Soc.* **1987**, *109*, 3945–3953.

(29) Bernatis, P.; Laurie, J. C. V.; Rakowski DuBois, M. *Organometallics* **1990**, *9*, 1607.

values of 2.6, 7.6, and 9.6, respectively, in acetonitrile.<sup>28,30</sup> The catalytic data discussed previously and shown in Figures 1–4 are for the acid *p*-cyanoanilinium tetrafluoroborate, but very similar results are also obtained when (CpMoS)<sub>2</sub>(S<sub>2</sub>CH<sub>2</sub>) is reduced in the presence of excess triflic acid (Figure S3). Catalytic waves are observed with both of these acids with half-wave potentials of –0.57 and –0.59 V for triflic acid and *p*-cyanoanilinium tetrafluoroborate, respectively. In the catalytic reactions with excess triflic acid, an irreversible reduction wave is observed at –0.4 V, which is attributed to the reduction of the iminothiolate dication **4**. The similarity of the subsequent catalytic wave at –0.57 V to that of the *p*-cyanoanilinium system suggests that the initial stoichiometric reduction promotes nitrile deinsertion from **4** and regeneration of **3** and that **3** is the active catalyst in both acid systems. This is further supported by our studies of solvent variation, discussed next. When *p*-bromoanilinium triflate is used as the acid (p*K*<sub>a</sub> = 9.6), the reduction wave occurs at more negative potentials (–0.73 V), and the *i*<sub>c</sub>/*i*<sub>p</sub> ratio is reduced from 2.8 to 1.7 at scan rates of 50 mV/s (Figure S4). In addition, for this acid, the solutions remain blue, the color of the unprotonated complex **2**. These data are fully consistent with only partial protonation of **2** in the presence of excess bromoanilinium.

When a 10-fold excess (as compared to the catalyst concentration) of a 1:1 mixture of *p*-cyanoanilinium/cyanoaniline is used in catalytic experiments under an atmosphere of hydrogen, the half-wave potential was observed to be –0.65 V versus ferrocene. Because the ratio of the acid and its conjugate base is one, the pH of this solution is equal to the p*K*<sub>a</sub> value of the acid, 7.6. The normal hydrogen electrode in acetonitrile occurs at a potential of –0.07 V versus the ferrocene/ferrocenium couple.<sup>31</sup> At our operating pH of 7.6, the thermodynamic potential for proton reduction in acetonitrile is calculated to be –0.53 V. The observed value of –0.65 V for this catalyst represents a very modest overpotential of 120 mV. The more negative potential observed when *p*-bromoanilinium is used as an acid is the result of the more negative potential required for proton reduction at a higher pH. As a result, the overpotential remains low, but the catalytic current as reflected in the *i*<sub>c</sub>/*i*<sub>p</sub> ratio is lower. The reduction of triflic acid occurs at a larger overpotential (approximately 350 mV) because of the mismatch in the pH of the solution and the p*K*<sub>a</sub> value of the catalyst, **3**, but the *i*<sub>c</sub>/*i*<sub>p</sub> ratio remains high. The results obtained using *p*-cyanoanilinium as the acid indicate that the optimum performance in terms of overpotential and catalytic rate is obtained when the p*K*<sub>a</sub> of the catalyst is matched to the pH of the solution.

**Solvent Dependence.** As described previously, the protonated complex **3** undergoes a further reversible reaction with acetonitrile in the presence of excess triflic acid, and this raises the question of the role of the solvent, acetonitrile, in the catalytic reaction. For this reason, the catalytic reaction was studied in 1,2-dichlorobenzene and dimethylformamide, in addition to acetonitrile. In 1,2-dichlorobenzene, the addition of excess triflic acid to **2** results in the formation of a red solution, consistent with the formation of **3**. In CV's recorded at 50 mV/s, the first reduction wave shifts from –1.80 to –0.58 V, increases in

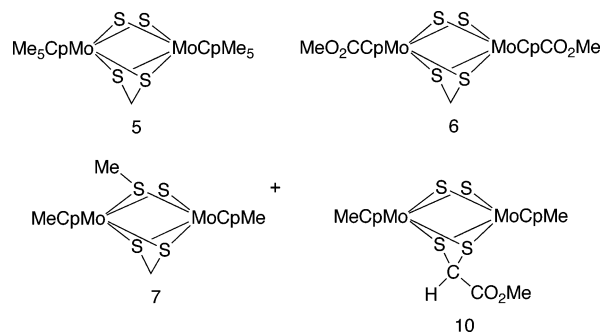


Figure 5. Substituted derivatives of **2** used in this paper.

height, and becomes irreversible with a shape characteristic of a catalytic current (Figure S5). In addition, as the acid concentration is increased, the reversible waves associated with **2** are no longer observed. This behavior is very similar to that observed in acetonitrile with both triflic acid (Figure S3) and *p*-cyanoanilinium (Figure 1). Hence, it is clear that the formation of the iminothiolate dication is not required for catalysis, and the data suggest that the protonated complex **3** is the active catalyst in each case. The *i*<sub>cat</sub>/*i*<sub>p</sub> ratios at a scan rate of 50 mV/s for **2** in 0.02 M triflic acid solutions of acetonitrile and 1,2-dichlorobenzene are 2.8 and 2.0, respectively. This ratio provides a comparison of the catalytic efficiency in the two solvents.

When **2** is protonated with *p*-cyanoanilinium ion in dimethylformamide, the first cathodic wave shifts from –1.66 to –1.18 V, and a small catalytic current is observed (*i*<sub>cat</sub>/*i*<sub>p</sub> = 1.3), but the color of the solution remains blue. No significant change is observed when excess triflic acid is added to this solution. From these data, it appears that **2** is not protonated to a significant extent in dimethylformamide. This is not surprising given the strong solvating properties of dimethylformamide for protons.<sup>31a</sup>

**Dependence on Cp Ring Substituents.** The electrocatalytic behavior of several derivatives of **2** shown in Figure 5 has been studied. To determine the influence of electron-donating and -withdrawing substituents on the cyclopentadienyl ring, cyclic voltammograms were recorded on **5** and **6** in acidic and nonacidic acetonitrile solutions. The Cp\* derivative, **5**, readily protonates in acetonitrile as indicated by a change in color from blue to red upon the addition of the *p*-cyanoanilinium ion. The first cathodic wave is shifted from –1.89 to –0.68 V as acid is added, and a wave characteristic of catalytic current is observed. However, the *i*<sub>c</sub>/*i*<sub>p</sub> ratio of 1.8 at a scan rate of 50 mV/s is less than the 2.8 value observed for **2**.

A reversible cathodic wave is observed at –1.40 V for the ester-substituted derivative **6** in the absence of acid. No color change is observed when excess *p*-cyanoanilinium ion is added, although two new irreversible waves are observed at *E*<sub>p</sub> = –0.59 and –0.96 V. In the presence of excess triflic acid, a single irreversible cathodic wave is shifted to –0.35 V. However, evidence for a significant catalytic current is not observed in the presence of either acid. These results indicate that the basicity and reactivity at the sulfido ligands in the dimers are quite sensitive to the electronic influence of the Cp substituents.

**Dependence on Sulfur Ligand Substituents.** To probe the role of the bridging sulfido ligands in H<sub>2</sub> production, the methanethiolate cation **7** was evaluated for catalytic activity. A voltammogram of **7** is shown in the red trace of Figure 6. Two reversible one-electron reduction waves are observed at –0.74

(30) Izutsu, K. *Acid–Base Dissociation Constants in Dipolar Aprotic Solvents*, IUPAC Chemical Data Series, No. 35; Blackwell Scientific Publications: Oxford, 1990.

(31) (a) Wayner, D. M.; Parker, V. D. *Acc. Chem. Res.* **1993**, *26*, 287–294. (b) Ellis, W. W.; Raebiger, J. W.; Curtis, C. J.; Bruno, J. W.; DuBois, D. L. *J. Am. Chem. Soc.* **2004**, *126*, 2738–2743.

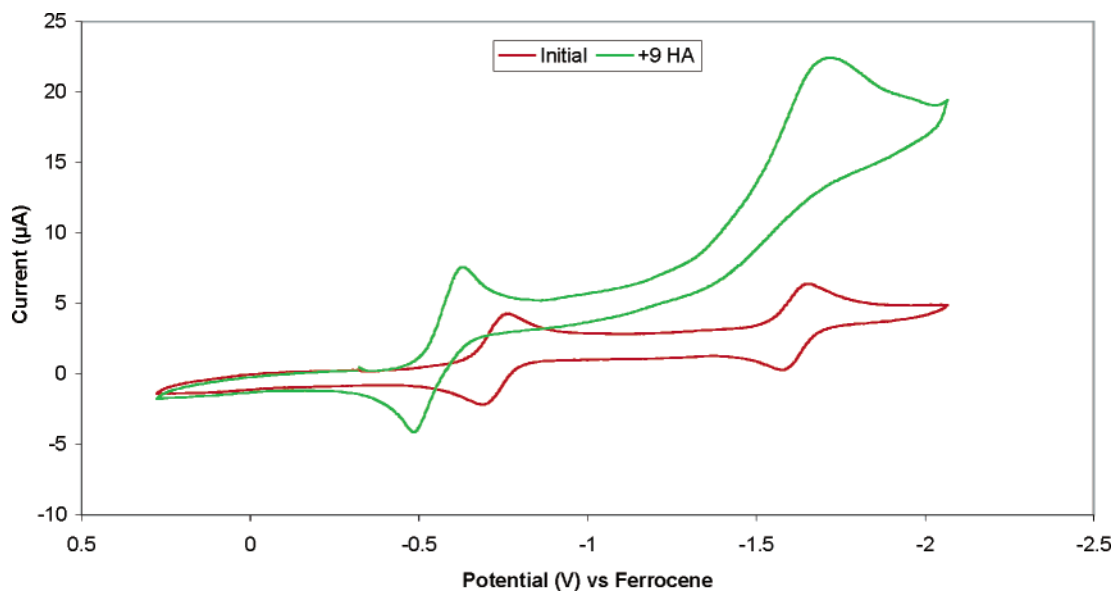
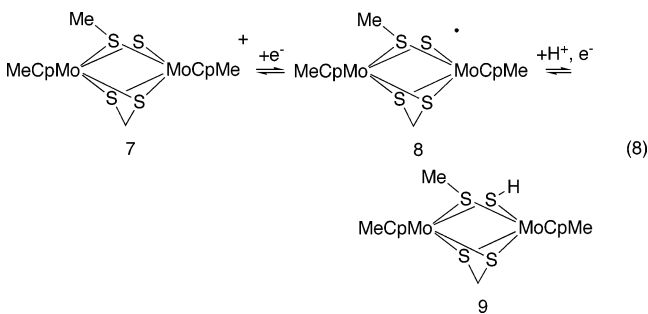


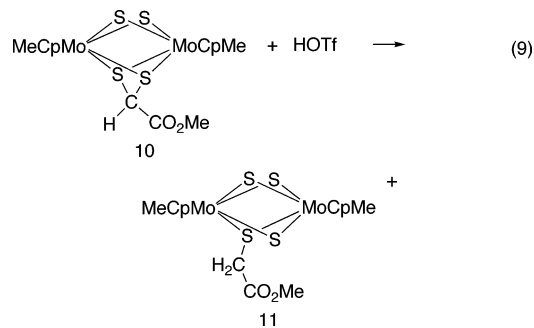
**Figure 6.** Cyclic voltammograms of  $[(\text{MeCpMo})_2(\text{S}_2\text{CH}_2)(\mu\text{-S})(\mu\text{-SMe})]\text{OTf}$ , **7** (0.97 mM), in the absence and presence of *p*-cyanoanilinium tetrafluoroborate recorded in 0.3 M  $\text{Et}_4\text{NBF}_4$  acetonitrile solution at a glassy carbon electrode at 50 mV/s.

V ( $\Delta E_p = 80$  mV) and  $-1.63$  V ( $\Delta E_p = 90$  mV). In previous work, both one-electron and two-electron reduction products of **7** have been prepared and their reactivities studied.<sup>17,32</sup> The first half-wave potential for **7** is similar to the potential of the first reduction wave observed for **3** in acetonitrile. Addition of 1 equiv of acid to an acetonitrile solution of **7** results in a new wave at  $-0.57$  V that shows an increase in the cathodic current by a factor of ca. 1.8 and a larger  $\Delta E_p$  value of 165 mV at a scan rate of 50 mV/s. Continued addition of acid has no further effect on this wave, and it remains diffusion-shaped with a fully developed anodic wave as shown in the green trace in Figure 6. The second irreversible reduction wave at  $-1.6$  V is attributed to the uncatalyzed reduction of the *p*-cyanoanilinium ion. The absence of a plateau-shaped current profile for the wave at  $-0.57$  V indicates that **7** displays no catalytic activity for proton reduction. The electrochemical results are consistent with an ECE reaction and the formation of the previously characterized Mo(III)/(III) dimer **9**<sup>32</sup> as shown in reaction 8. During the return anodic scan, this species is oxidized, and the reverse ECE sequence is observed.



The effect of a substitution on the methanedithiolate ligand has been studied using complex **10** in Figure 5. Although the methanedithiolate ligand in **2** and related derivatives is inert to acid, the addition of acid to complex **10** has been found to result

in the cleavage of a carbon sulfur bond of the 1,1-dithiolate ligand and the formation of **11** (eq 9).<sup>33</sup>



When the cyclic voltammogram of **10** is run in the presence of excess (28 equiv) triflic acid, the cathodic wave shifts from  $-1.59$  to  $-0.52$  V, and a plateau shaped current with an  $i_c/i_p$  ratio of 3.5 indicates that the protonated complex is an active catalyst for proton reduction (Figure S7). Our studies of the various methanedithiolate derivatives indicate that increasing the number of alkylated sulfur bridges eliminates the catalytic activity that is observed for **2**, while derivatives with two or three unsubstituted sulfido ligands function as active catalysts in the presence of protons.

Cyclic voltammograms of  $[\text{CpMo}(\mu\text{-S})(\mu\text{-SH})_2]$ , **1**, in acidic acetonitrile solutions do not exhibit catalytic waves near  $-0.6$  V as observed for **2**. A less facile proton reduction process is indicated for **1** with a catalytic wave observed at the more negative potential of  $-0.96$  V (Figure 6S). Hydrogen was identified as the product of the reduction in a bulk electrolysis experiment, but additional studies were not carried out on hydrogen evolution with this system.

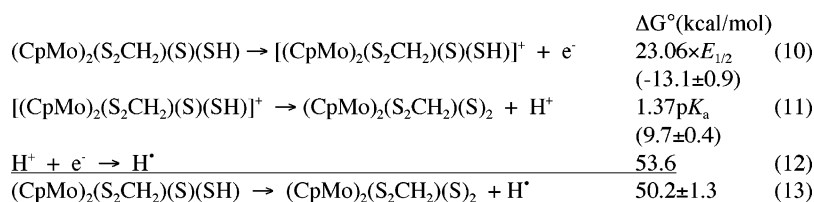
**Thermodynamic Studies.** The availability of the  $\text{p}K_a$  value for **3** and of the redox potentials for its conjugate base, **2**, in acetonitrile permit us to derive some additional thermodynamic

(32) Casewit, C. J.; Rakowski DuBois, M. *J. Am. Chem. Soc.* **1986**, *108*, 5482.

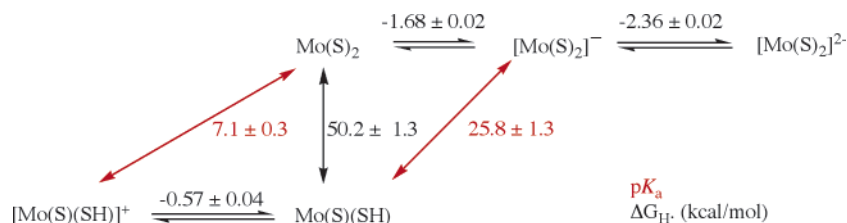
(33) Lopez, L. L.; Gabay, J.; Haltiwanger, R. C.; Green K.; Allshouse, J.; Casewit, C.; Rakowski DuBois, M. *Organometallics* **1993**, *12*, 4764.



## Scheme 1



## Scheme 2



data for the S–H bond in dinuclear hydrosulfido complexes. The sum of reactions 10–12 shown in Scheme 1 can be used to calculate the homolytic bond dissociation free energy of the mixed-valence derivative  $(\text{CpMo})_2(\text{S}_2\text{CH}_2)(\text{S})(\text{SH})$  in acetonitrile (reaction 13). The free energy associated with each reaction is listed in parentheses immediately following the reaction. The potential of the  $[(\text{CpMo})_2(\text{S}_2\text{CH}_2)(\text{S})(\text{SH})]^+ / (\text{CpMo})_2(\text{S}_2\text{CH}_2)(\text{S})(\text{SH})$  couple shown in reaction 10 was determined from the potential at half-height for the catalytic wave of  $[(\text{CpMo})_2(\text{S}_2\text{CH}_2)(\text{S})(\text{SH})]^+$ , which is equal to the half-wave potential.<sup>26</sup> The  $\text{p}K_a$  of  $7.1 \pm 0.3$  for  $[(\text{CpMo})_2(\text{S}_2\text{CH}_2)(\text{S})(\text{SH})]^+$  was determined as described above, and the value of 53.6 kcal/mol for the free energy of the reduction of a solvated proton in acetonitrile is taken from the literature.<sup>31</sup> Summation of the free energies associated with reactions 10–12 gives a homolytic bond dissociation free energy of  $50.2 \pm 1.3$  kcal/mol for the S–H bond in  $(\text{CpMo})_2(\text{S}_2\text{CH}_2)(\text{S})(\text{SH})$ . Because homolytic bond dissociation enthalpies are expected to exceed bond dissociation free energies by approximately 5 kcal/mol,<sup>31a</sup> this gives an estimated S–H bond energy of 55 kcal/mol for  $(\text{CpMo})_2(\text{S}_2\text{CH}_2)(\text{S})(\text{SH})$ .

This value is significantly lower than the gas-phase value calculated for the stable hydrosulfide complex **1** (73 kcal/mol),<sup>34</sup> which is, in turn, lower than those reported for organic thiols and  $\text{H}_2\text{S}$  (ca. 78–92 kcal/mol).<sup>35</sup> A similar cycle can be used to determine a  $\text{p}K_a$  value of  $25.8 \pm 1.3$  for  $(\text{CpMo})_2(\text{S}_2\text{CH}_2)(\text{S})(\text{SH})$  (see Supporting Information for the thermodynamic cycle used). The thermodynamic relationships between the different molybdenum species are shown in Scheme 2. In Scheme 2, Mo represents the fragment  $(\text{CpMo})_2(\text{S}_2\text{CH}_2)$ . The horizontal equilibrium arrows represent reversible one-electron-transfer processes, and the corresponding potentials are listed above the arrows. Black vertical arrows represent homolytic bond dissociation free energies. Red diagonal arrows indicate deprotonation reactions with the corresponding  $\text{p}K_a$  values shown in red type. From these data, it can be seen that reduction of  $[(\text{CpMo})_2(\text{S}_2\text{CH}_2)(\text{S})(\text{SH})]^+$  to  $(\text{CpMo})_2(\text{S}_2\text{CH}_2)(\text{S})(\text{SH})$  results in an increase in the  $\text{p}K_a$  value that corresponds to a 25 kcal/mol increase in energy. The homolytic bond dissociation free energy of 50.2 kcal/mol for the S–H bond in  $(\text{CpMo})_2-$

$(\text{S}_2\text{CH}_2)(\text{S})(\text{SH})$  is sufficiently low that a bimolecular elimination of dihydrogen is thermodynamically favorable. That is, the sum of two SH bond dissociation free energies (100 kcal/mol) is less than the free energy associated with  $\text{H}_2$  cleavage in acetonitrile (103.6 kcal/mol).<sup>31a</sup>

## Discussion

The results described in this paper demonstrate that **2** is a very selective catalyst (or catalyst precursor) for the electrochemical reduction of protons to hydrogen with a current efficiency of close to 100%. In addition, the relationships observed between acid strength, catalytic currents, and the reduction potentials indicate that the catalyst is capable of operating at very modest overpotentials (120 mV) when the acid strength is selected to match the  $\text{p}K_a$  value of **3**. These two results, high current efficiency and low overpotentials, indicate that **2** can exhibit high energy-conversion efficiencies for  $\text{H}_2$  production. In future work, it may also be possible to develop this class of compound as electrocatalysts for hydrogen oxidation, and in this context, it is important to note that the catalytic performance of the system is not strongly inhibited by CO, a contaminant commonly observed in crude hydrogen sources that inhibits platinum catalysts.<sup>36</sup> On the basis of previous studies of the stability of this class of compounds in the presence of  $\text{H}_2\text{S}$  and other organosulfur compounds, inhibition by sulfur-containing compounds is also unlikely.<sup>12,16</sup> These results all indicate that this class of catalysts possesses very attractive features as hydrogen production and potential oxidation catalysts. The hydrogen evolution promoted by these homogeneous catalysts presents a potential model for reactions of molybdenum sulfide surfaces.  $\text{MoS}_2$  on graphite has been found to catalyze hydrogen evolution with an overpotential of 100–200 mV at  $\text{pH} = 0$ .<sup>17f</sup>

The catalytic activity for proton reduction was studied with several substituted derivatives of **2** to obtain information about electronic and structural factors that influence the catalytic reaction. Varying Cp ring substituents alters the  $\text{p}K_a$  of the complex and can also affect the reactivity of the complex in its cationic protonated form. It appears that a rather sensitive balance between sulfur basicity in the neutral derivative and electrophilicity in the protonated cation is required for maximum catalytic proton reduction activity to be observed. In addition,

(34) Franz, J. A.; Birnbaum, J. C.; Kolwaite, D. S.; Linehan, J. C.; Camaioni, D. M.; Dupuis, M. *J. Am. Chem. Soc.* **2004**, *126*, 6680.

(35) (a) Bordwell, F. G.; Zhang, X. M.; Satish, A. V.; Cheng, J. P. *J. Am. Chem. Soc.* **1994**, *116*, 6605. (b) Bensen, S. *Chem. Rev.* **1978**, *78*, 23.

(36) Ralph, T. R.; Hogarth, M. P. *Platinum Met. Rev.* **2002**, *46*, 117.

the extent of alkyl substitution on the sulfur ligands was found to be a critical factor in the catalytic activity. Methylation of one of the sulfido ligands of **2** to form **7** completely eliminates the catalytic formation of hydrogen. Studies of the solvent dependence indicate that catalytic proton reduction occurs in both acetonitrile and dichlorobenzene, but strongly basic solvents such as DMF inhibit the protonation of **2** required for catalytic activity.

The mechanism of this hydrogen production reaction was probed to better understand the factors controlling the catalytic rate. At low acid concentrations, the catalytic current is proportional to the acid concentration, consistent with either a preequilibrium followed by a catalytic reaction or with a rate-determining step that is second order in acid. On the basis of our  $pK_a$  measurements, the former seems more likely. At higher acid concentrations, the rate is independent of the acid concentration and first order in catalyst concentration. This is interpreted as a rate-limiting dissociation of  $H_2$  from a dinuclear molybdenum intermediate. This is the reaction that must be enhanced for catalysts such as **2** to achieve much higher catalytic rates, and studies are in progress to achieve a better understanding of the mechanism of hydrogen elimination and of the factors that promote it.

Although the intermediate  $(CpMo)_2(S_2CH_2)(\mu-S)(\mu-SH)$ , formed upon a one-electron reduction of **3**, is thermodynamically capable of eliminating dihydrogen in a bimolecular reaction as discussed above, the first-order dependence on catalyst is not consistent with this pathway. Additional mechanisms for the reversible elimination of dihydrogen from either a neutral or cationic intermediate have been described in the Introduction. For example, a catalytic cycle can be envisioned that involves the net addition of two electrons and two protons to **2** to form the proposed neutral product of reaction 3, which is expected to readily eliminate hydrogen. Hydrogen elimination could also occur from a cationic intermediate as shown in reaction 4. Hydrogen elimination from two adjacent hydrosulfido ligands, as shown in path a, would resemble a reductive elimination from a transition metal dihydride.<sup>13a</sup> Elimination from a hydrosulfido ligand and a molybdenum hydride in a cationic intermediate, reaction 4, path b, would be the reverse of the heterolytic activation of hydrogen. Density functional calculations for the pathways in reaction 4 indicate that either transition state is at least 45 kcal/mol above the reactant and products.<sup>37</sup> Although solvent effects are not taken into account in the calculations, such a large activation barrier does not appear to be consistent with the observed catalytic rate, and this suggests that hydrogen elimination from a neutral intermediate is occurring in this system. Calculations that compare the elimination pathways for the neutral and ionic intermediates would be of interest. Our observation that the methanethiolate cation, **7**, does not function as a catalyst for hydrogen formation also appears to favor elimination from a neutral catalytic intermediate. Investigations of the spectroscopic properties of **2** and **3** under high pressures of hydrogen may provide further insights into the nature of the intermediates involved. In addition, synthetic modifications of the dimers that may increase the rate of hydrogen elimination, and which will enable the catalytic reaction to be studied in aqueous solutions as well as on solid supports, will be explored.

## Conclusion

The high current efficiency and low overpotentials observed for **2** in the electrocatalytic production of  $H_2$  indicate that this catalyst can exhibit high energy-conversion efficiencies for this process. In addition, the catalytic performance of **2** is not strongly inhibited by CO, a characteristic that will be important in the development of related electrocatalysts for the reverse process, hydrogen oxidation. Kinetic studies of **2** and several related complexes are consistent with the reductive elimination of  $H_2$  from a binuclear complex as the rate-determining step. The results of this work demonstrate that hydrogen production catalysts based on soluble metal sulfides can produce hydrogen with the involvement of hydrosulfido ligands.

## Experimental Procedures

**Materials and Instrumentation.** The molybdenum dimers used in this work,  $[CpMo(\mu-S)(\mu-SH)]_2$ ,<sup>12</sup>  $(CpMo\mu-S)_2S_2CH_2$ ,<sup>14</sup>  $(Cp^*Mo\mu-S)_2S_2CH_2$ ,<sup>27</sup>  $(MeO_2CCpMo\mu-S)_2S_2CH_2$ ,<sup>38</sup>  $(MeCpMo)_2(\mu-S)(\mu-SMe)(S_2CH_2)]-OTf$ ,<sup>18</sup> and  $(MeCpMo\mu-S)_2(S_2CHCO_2Me)$ ,<sup>33</sup> were synthesized by published procedures. Triflic acid, *p*-cyanoaniline, and *p*-bromoaniline were purchased from Aldrich. *p*-Cyanoanilinium tetrafluoroborate was synthesized by the addition of fluoroboric acid (48% aq, 1.6 mL, 0.012 mol) to a filtered solution of *p*-cyanoaniline (1.20 g, 0.010 mol) in ether (90 mL). The protonated salt that precipitated from solution was filtered, washed with ether, and dried in vacuo. A similar procedure with triflic acid was used in the synthesis of *p*-bromoanilinium triflate. Acetonitrile was distilled from calcium hydride.

Electrochemical data were collected using a Cypress System model CS-1200 computer-aided three-electrode electrolysis system.  $^1H$  NMR data were obtained on a Varian Inova 500 MHz instrument.

**Catalytic Proton Reduction.** Cyclic voltammetry was used to evaluate the catalytic activity of **2** and related compounds for proton reduction. The working electrode was a glassy carbon disk, the counter electrode was a glassy carbon rod, and an electrode consisting of a silver wire coated with AgCl was used as a pseudo-reference electrode. Ferrocene was used as an internal standard, and all potentials are referenced to the ferrocene/ferrocenium couple. Catalyst was added to an acetonitrile solution containing 0.3 M  $Et_4NBF_4$  to make the solution 0.95 mM in catalyst. The solution was purged with  $N_2$ , and an initial cyclic voltammogram was recorded. Aliquots of 0.18 M acid in the electrolyte solution were added, and the cyclic voltammograms were recorded at a scan rate of 50 mV/s to determine the catalytic currents.

**Kinetics of the Catalytic Reaction.** Similar cyclic voltammetry experiments were used to determine the kinetics of the catalytic reaction. The order with respect to acid was determined by titration with *p*-cyanoanilinium tetrafluoroborate (0.18 M in electrolyte solution) and plotting the resulting values of  $i_c/i_p$  versus  $[H^+]$ . The peak current observed under 1 atm  $N_2$  in the absence of acid is  $i_p$ , and the peak or plateau current observed in the presence of various amounts of acid is  $i_c$ .

To determine the catalyst dependence, aliquots of a 0.95 mM stock solution of the catalyst in acetonitrile were added to *p*-cyanoanilinium tetrafluoroborate (9.5 mM in electrolyte solution). Additional aliquots of the stock acid solution (0.18 M) were also added to maintain a constant concentration of acid despite dilution. Cyclic voltammograms were recorded at a scan rate of 50 mV/s after each addition, and a plot of the plateau current versus the catalyst concentration was used to determine the order with respect to catalyst.

**Cyclic Voltammetry under CO.** The solution of **2** (0.95 mM) was purged with pure carbon monoxide for 20 min, then cyclic voltammograms of the solution were recorded as aliquots of *p*-cyanoanilinium tetrafluoroborate (0.18 M) were added as described previously.

(37) McGrady, J. E.; Budria, J. G. *J. Organomet. Chem.*, in press; and private communication.

(38) Allshouse, J.; Kaul, B. B.; Rakowski DuBois, M. *Organometallics* **1994**, *13*, 28.

**Solvent Dependence.** Cyclic voltammograms were recorded on **2** (0.86 mM) in DMF containing 0.3 M Et<sub>4</sub>NBF<sub>4</sub> as aliquots of *p*-cyanoanilinium tetrafluoroborate (0.17 M in the electrolyte-containing solution) were added. Similarly, cyclic voltammograms were recorded on **2** (1.1 mM) in 1,2-dichlorobenzene containing 0.3 M Bu<sub>4</sub>NBF<sub>4</sub> as aliquots of triflic acid (0.23 M in the electrolyte-containing solution) were added.

**Bulk Electrolysis of **2** with Excess Acid.** Complex **2** (0.012 g, 0.026 mmol) and *p*-cyanoanilinium tetrafluoroborate (0.153 g, 0.74 mmol) were dissolved in 23 mL of CH<sub>3</sub>CN containing 0.3 M Et<sub>4</sub>NBF<sub>4</sub>. The solution was electrolyzed under nitrogen in a sealed three-compartment electrochemical cell with a volume in the working compartment of 143 mL. The electrolysis was carried out at a reticulated vitreous carbon electrode (1 cm diameter by 2.5 cm length, 60 pores/in.) at -0.960 V versus ferrocene for 3 h with the consumption of 52.8 C (5.5 × 10<sup>-4</sup> F). A syringe was used to withdraw gas from the headspace of the cell, and the gas was confirmed to be a hydrogen/nitrogen mixture by analysis with a gas chromatograph using a thermal conductivity detector. By comparison with a standard calibration curve, the gas was determined to be 6.7% hydrogen. A yield of 2.7 × 10<sup>-4</sup> mol of H<sub>2</sub> was calculated for *T* = 22 °C and *P* = 0.824 atm (Boulder, CO) for a current efficiency of 98%.

**Reactions of **3** with Acid in Acetonitrile.** The NMR spectra of CD<sub>3</sub>CN solutions of **2** containing from 1 to 6 equiv of triflic acid were recorded after 20 min and after ca. 20 h. The spectrum with 1 equiv of acid showed rapid proton exchange between **2** and **3** with nearly quantitative formation of **3**. After the addition of 2 equiv of acid, the spectrum showed discrete resonances for the nitrile insertion product **4**<sup>29</sup> (ca. 30%) as well as for **3**. With additional equivalents of acid, **3** disappeared, and **4** (72%) as well as a second unidentified product (28%, NMR: 6.98, 6.92 2s, Cp; 4.6 AB pattern, S<sub>2</sub>CH<sub>2</sub>) was observed in the spectrum. The addition of triethylamine to these solutions reversed the reactions and reformed **2**.

The NMR spectrum of a CD<sub>3</sub>CN solution of **2** with 4.4 equiv of *p*-cyanoanilinium tetrafluoroborate was recorded after 20 min. The chemical shifts were consistent with a mixture of ca. 77% protonated complex **3** and 23% **2**. No evidence for the formation of **4** was observed. The spectrum was recorded again after ca. 20 h, and no significant change was observed.

**Determination of p*K*<sub>a</sub> of **3**.** In a typical experiment, **2** (0.0065 mmol), *p*-cyanoaniline (B) (0.13 mmol), and *p*-cyanoanilinium tetrafluoroborate (HB) (0.26 mmol) were dissolved in ca. 1 mL of CD<sub>3</sub>CN under nitrogen, and the NMR spectrum was recorded after ca. 20 min. The chemical shifts of the pure protonated complex **3** are 6.95 (Cp) and 4.00 ppm (S<sub>2</sub>CH<sub>2</sub>) and for the deprotonated complex **2**, 6.49 and 2.76 ppm. In the presence of the excess acid/base, rapid exchange was observed between these two species, and chemical shifts of 6.64 and 3.23 ppm were observed. Determination of the ratio of **3**/2 × [B]/[HB] gave a *K* for the protonation of **2** of 0.3. The addition of log *K* to the p*K*<sub>a</sub> value for *p*-cyanoanilinium (7.6) gave a p*K*<sub>a</sub> for **3** of 7.1 in acetonitrile.

**Acknowledgment.** This work was supported by a grant from the National Science Foundation. D.L.D. acknowledges support from the U.S. Department of Energy, Office of Science, Chemical and Biological Sciences Division, under DOE Contract DE-AC36-99G010337.

**Supporting Information Available:** Cyclic voltammograms for **1** and derivatives of **2** as a function of acid concentration for various acids and solvents; thermodynamic data used in the calculation of the p*K*<sub>a</sub> of (CpMo)<sub>2</sub>(S<sub>2</sub>CH<sub>2</sub>)(μS)(μ-SH). This material is available free of charge via the Internet at <http://pubs.acs.org>.

JA054034O